

Precision, High Stability High Voltage Module Power Supply for Analytical Instrumentation

Sunil Kumar Sahu, P. G. Abichandani and S. Malhotra

Electromagnetic Application and Instrumentation Division, Bhabha Atomic Research Centre, Mumbai - 400085, Maharashtra, India; ssahu@barc.gov.in

Abstract

Analytical instruments like mass spectrometer¹⁻⁴ require a highly stable environment for precise measurements. A minute fluctuation in supply can cause large errors in measurements. For accelerating the ions in a mass spectrometer, a highly stable high-voltage power supply is required. High voltage power supplies up to 30kV/10W with 10ppm short-term stability are extensively used in various analytical instruments like mass spectrometers, PMT and CEM, scanning electron microscope, electron spectroscopy etc. This paper will illustrate the design concept and implementation of an HV module based on a compound regulatory system, where a linear regulator feeds the power to the switching regulator (ZVS mode resonance converter fly-back topology, SMPS) operating around 100 kHz.

Keywords: Electron Spectroscopy, Mass Spectrometer, ZVS Mode Resonance Converter

1. Introduction

In a precision power supply, where regulation of a very high order is required, a very high gain error amplifier is used to detect minute changes in the power supply's output. Noise considerations play a major role in the design of such a circuit. Also, the output voltage drift must be minimized against temperature changes. Hence the design must include precision, ultra-stable components, minimum noise and ringing due to switching elements and minimum power dissipation across the components. In a compound regulatory power supply system, the cascading of a series regulator stage to a DC-to-DC resonant converter results in a simplified design which combines the benefits of both the linear and ZVS techniques of SMPS. The block diagram of the power supply is given in Figure 1.

The objective of this project was to design a precision, high stability 50ppm high voltage module for various analytical instruments with specifications as shown in Table 1.

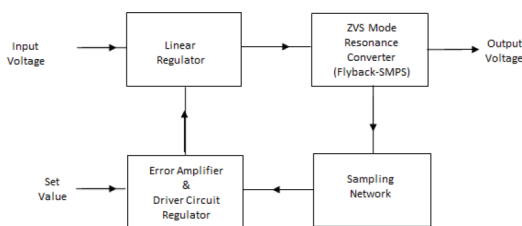


Figure 1. Block diagram.

Table 1. Specification of the power supply

Parameter	Specification
Input voltage	24V \pm 1V,
Output voltage	0V up to 30kV
Maximum power	10W
Ripple and noise	300mV (p-p),
Stability	50ppm for 8 Hours
Line regulation	0.001% (\pm 1V input change)
Load regulation	0.001% (10% to 100%load)
Protection	Arc, overload/over the current and short circuit with self-recovery type

*Author for correspondence

2. Design Approach

2.1 Linear Regulator

The block diagram of a linear regulator is shown in Figure 2. As the source voltage or load resistance varies, the effective resistance of the series pass element is increased or decreased, such that it absorbs the change in source voltage/load current.

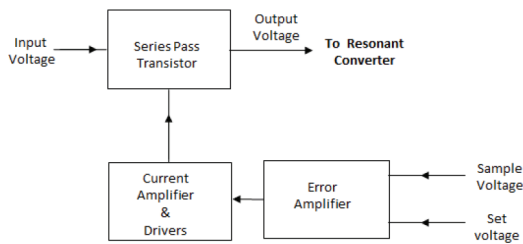


Figure 2. Linear regulator.

Controlling of the series-pass transistor(s) is accomplished by the negative feedback loop which consists of a highly stable precision reference signal from IC REF 10, a precision sampling network and a low drift error amplifier and driver.

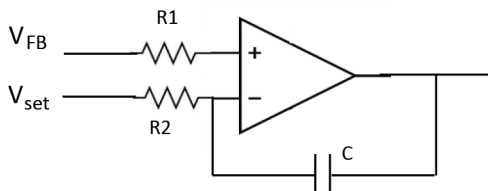


Figure 3. Error amplifier.

The differential error amplifier (Figure 3) is defined as a precision low-offset op-amp. The transfer function of error amplifier^{5,6} is given by $\frac{1+R_1CS}{R_1CS}$. In this configuration error amplifier has a pole at origin which determines the open loop gain of the op-amp for DC and helps to achieve a highly regulated power supply.

As output tends to change, either because of changes in output load current or input voltage, the differential error amplifier compares the output sample voltage with a reference voltage and produces an error signal. This signal, after further amplification by the driver/level shifter, changes the base current of the series pass transistor in such a way that the output voltage is kept at a constant level.

2.2 Zvs Mode Resonant Converter

Figure 4 shows the circuit diagram of the flyback converter and its equivalent circuit^{7,8}. The equivalent

circuit of a flyback converter consists of a leakage inductor (L_l) and magnetizing inductor (L_m) of the transformer, lump capacitance (C_{Lump}) lump capacitance is the sum of the parasitic capacitance of transformer winding (C_t), parasitic capacitance of drain-source of the mosfet (C_{ds}) and reflected capacitance of the secondary diode ($N^2.C_D$).

$$C_{Lump} = C_t + C_{ds} + N^2.C_D \quad (1)$$

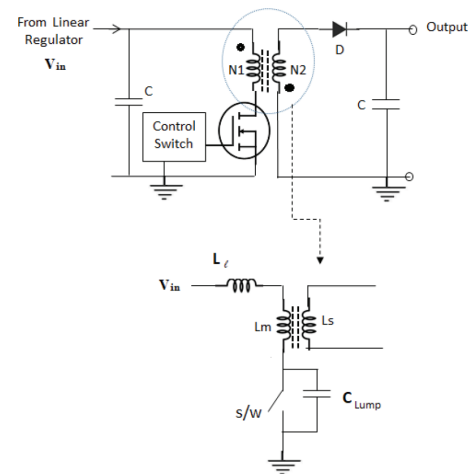


Figure 4. Flyback converter and its equivalent circuit.

PWM controller IC3525 is used to generate a 100kHz switching waveform. In a flyback converter, during the power transistor 'on' period the dot end of the winding is positive concerning the non-dot end. Hence output rectifier diode is reverse-biased, and the output load current is supplied from the output storage capacitors only. During the turnaround time-on, here is the fixed voltage across the primary wing, since the secondary winding is in an open loop configuration with primary winding as an inductor and the current ramps up linearly⁵⁻⁷ at the rate of $\frac{di}{dt} = \frac{V_m}{L_p}$ where L_p is the primary inductance. At the end of the other n time the primary current has ramped up to $I_p = \frac{(V_{in} - V_o)T_m}{L_p}$. The observed switching waveform on oscilloscope is shown in Figure 5.

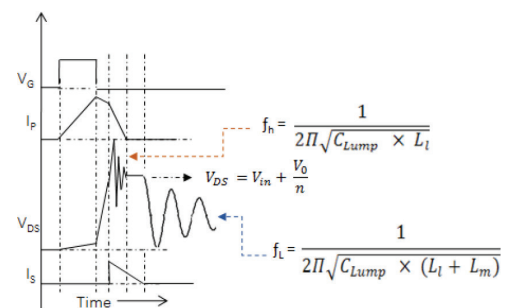


Figure 5. Switching waveforms.

This current represents stored energy of $E = \frac{1}{2} L_p I_p^2$ per cycle. When the transistor turns off, the mosfet forces the magnetization current to drop to zero, magnetizing current reverses the polarity of the transformer coils, now the non-dot end of the transformer becomes positive, and the lump capacitor starts to charge with the energy stored in the leakage and magnetization inductor. The drain-source voltage⁷ is given by:

$$V_{DS} = V_{Clump} = \frac{1}{C_{lump}} \int_0^t i(t) dt \quad (2)$$

When the potential across lump capacitor (i.e. drain-source voltage of mosfet) exceeds the potential sum of input voltage and the equivalent bk emf ($\frac{V_o + V_d}{N}$) of output voltage, the diode in the secondary side becomes forward biased. The moment the secondary current starts to flow, the energy stored in the magnetizing inductor is transferred to the secondary side. Now the energy present in the leakage inductor keeps on charging the lump capacitor, the leakage inductor and lump capacitor form an LC resonant tank circuit and give a high frequency ringing as seen in the drain waveform. The energy stored in the leakage inductor is partially transferred to charge the lumped capacitor and the remaining energy is dissipated to the LC tank circuit as high-frequency ringing. The ringing frequency⁷ is given by:

$$f_h = \frac{1}{2\pi \sqrt{L_l \times C_{lump}}} \quad (3)$$

This ringing disappears once the energy stored in the leakage inductor is dissipated. After that, the drain-source voltage⁷ is given by:

$$V_{DS} = V_{in} + \frac{V_o + V_d}{N} \quad (4)$$

The secondary current ramps down lump to only ($\frac{dI_s}{dt} = \frac{V_o}{L_s}$) at constant voltage of V_o . When the secondary current dies out, the back emf ($\frac{V_o + V_d}{N}$) induced in the primary coil due to the secondary current reducing to zero. If the secondary current has ramped down to zero before the start of the next cycle (magnetizing energy stored in the primary when the power transistor was on, has been delivered to the secondary side) the circuit low-frequency operated in the discontinuous mode. But the lump capacitor has been charged up-to the voltage, $V_m + \frac{V_o + V_d}{N}$ (Equation 4). In this continuous lumped of operation (DCM), the lump capacitor forms an LC tank circuit with the leakage inductor along with the magnetizing inductor and gives a low frequency oscillation⁷ as given in Equation (5).

$$f_l = \frac{1}{2\pi \sqrt{(L_l + L_l) C_{lump}}} \quad (5)$$

Thus, energy stored in the leakage inductance gives a high-frequency ringing across the drain source and in the discontinuous mode of operation (DCM), the energy stored in the lumped capacitor gives a low-frequency oscillation across the drain source; ZVS mode operation is achieved by switching the MOSFET "ON" at the valley of low-frequency oscillation (i.e. zero voltage across the MOSFET while switching).

2.3 Output Section

Figure 6 shows the circuit diagram of the output section. It consists of a double circuit followed by an RC filter. The output voltage and a sample signal for regulating the output voltage are taken after the RC filter.

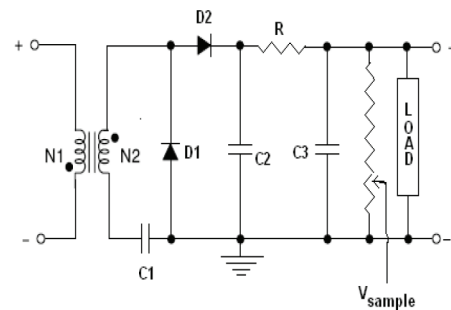


Figure 6. Output of the power supply.

3. Test Setup and Measurements

The 30kV HV module was connected to the 100MΩ resistive load, and the following measurements were taken.

- The reference signal was varied from 0V to 5V to get a regulated output from 0V to 30kV across the load.
- The output voltage was set to a fixed value and load regulation was measured with 10% to 100% load current change. The process was repeated for different voltages throughout the range.
- The line regulation was checked by varying the input voltage by $\pm 1V$. The process was repeated for different output voltages throughout the range.
- The most challenging measurement was the output ripple in the high-voltage power supply. It was measured by DC blocking techniques, where a

suitable C-R filter was used. The capacitor blocks the high voltage DC and passes the AC ripple which is observed on 36100 DCA Aplab 100MHz two-channel oscilloscope with a normal 1X probe.

The practical current and voltage waveforms of the MOSFET are shown in Figure 7. The output ripple waveform of 270mVp-p is shown in Figure 8. Practical waveforms closely follow the theoretical waveforms.

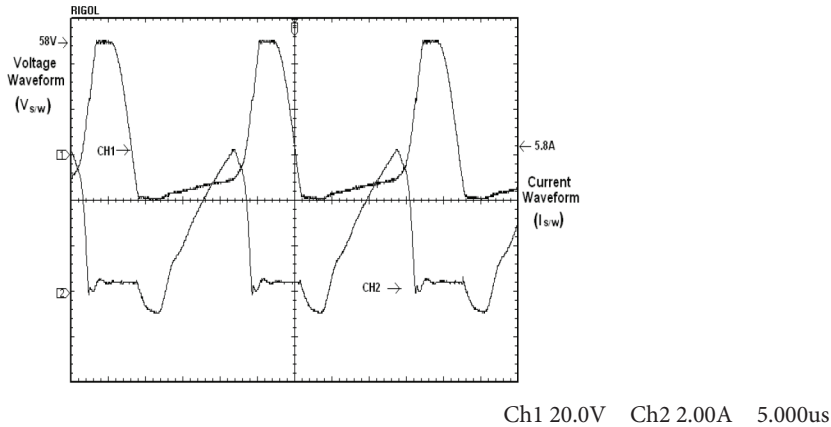


Figure 7. Practical current and voltage waveforms.

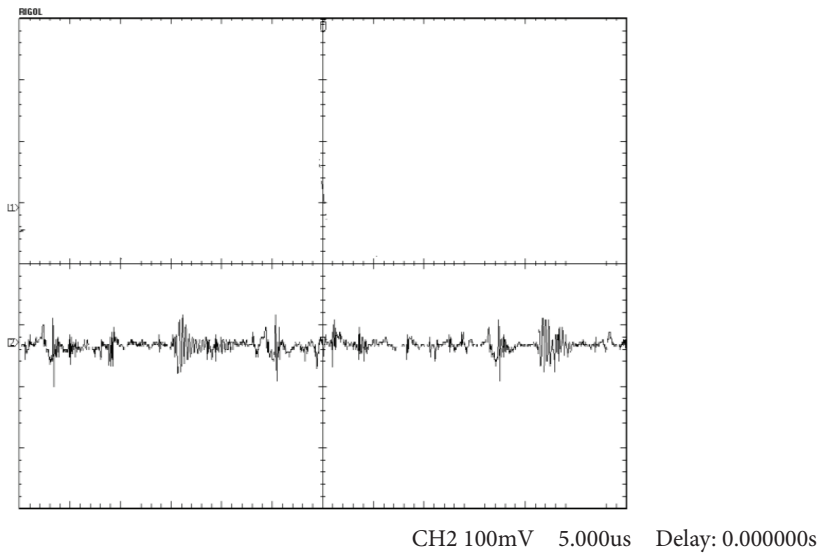


Figure 8. Output ripple 270mV(p-p) @30kV/0.3mA load current.

Summary of the result observed at the full voltage at full load as follows: a well-regulated variable output voltage from 50V to 30kV, corresponding 0 to 10V control signal; stability better than 40ppm for 8 hours; 0.0008%-line regulation for $\pm 1V$ input change; 0.001% load regulation for 10% to 100% load change and ripple less than 270mV (p-p) were obtained.

Based on the above techniques, HV modules of different voltage and current ratings up to 30kV/10W were developed.



Figure 9. 5kV/2mA and 10kV/1mA HV modules.



Figure 10. Polarity reversible 5kV/2mA and 30kV/0.3mA HV modules.

4. Conclusion

A precision power supply requires output noise and ripple to be ultra-low. It is observed that, in the fly-back converter, the ringing and oscillation across the drain source depend only on the circuit components and do not depend upon the operating conditions. So for a given duty cycle and switching frequency, a proper design of transformer with required leakage inductance, magnetizing inductance and parasitic capacitance, the ringing can be eliminated (which helps to design an ultra-low ripple/noise power supply) and by using ZVS mode of operation, turn on loss across the MOSFET can be reduced to zero (which helps to limit the temperature variation, enhance the efficiency and compactness of the power supply). The high stability is achieved by choosing a high stability component like a sampling network (5ppm/°C), low drift error amplifier (1.3uV/°C) and reference signal (2.5ppm/°C) used in the

feedback path. So, the design concept described herein has resulted in a precision (ultra-low ripple/noise), high stability compact high voltage module which will find extensive use in analytical instruments.

5. Acknowledgement

The authors are thankful to Shri Sanjay Malhotra, Head of, the Electromagnetic Application, and Instrumentation Division for their support in this development. The authors also express gratitude to Shri P G Abichandani, Shri. Nataraju, Shri R.K.Bhatia for their support.

6. References

1. Roboz J. Introduction to mass spectrometry: Instrumentation and techniques; 1968.
2. Aggarwal SK, Jain HC. Introduction to mass spectrometry; 1997.
3. Dawson PH. Quadrupole mass spectrometry and its applications. Elsevier; 2013.
4. Lorusso A, Siciliano MV, Velardi L, Nassisi V. Ion acceleration by a double-stage accelerating device for laser-induced plasma ions. *Radiation Effects and Defects in Solids: Incorporating Plasma Science and Plasma Technology*. 2010; 165(6-10):521-7. <https://doi.org/10.1080/10420151003722537>
5. Chetty PRK. Switch-mode power supply design. (No Title). 1986.
6. Pressman A. Switching power supply design. McGraw-Hill Education; 2009.
7. Basso CP. Switch-mode power supplies. McGraw-Hill Education; 2014.
8. Lu HY, Zhu JG, Hui SR. Experimental determination of stray capacitances in high-frequency transformers. *IEEE Transactions on Power Electronics*. 2003; 18(5):1105-12. <https://doi.org/10.1109/TPEL.2003.816186>